

Molecular Design for a Pinpoint RNA Scission. Interposition of Oligoamines between Two DNA Oligomers¹

Masayuki Endo, Yasushi Azuma, Yoshitaka Saga, Akinori Kuzuya, Gota Kawai, and Makoto Komiyama*

Department of Chemistry and Biotechnology, Graduate School of Engineering, The University of Tokyo, Hongo, Bunkyo-ku, Tokyo 113, Japan

Received June 24, 1996[®]

Phosphoramidite monomers having a benzyl or ethyl ester in the side chain have been synthesized for the facile and selective functionalization of oligonucleotides. Various amino compounds were incorporated into the desired sites in oligonucleotides by aminolysis of the esters. The conjugates, in which oligoamines (catalysts for RNA hydrolysis) were interposed between two oligonucleotides, hydrolyzed RNA substrates at exactly the target sites, which was consistent with the results of a computer-modeling study.

Introduction

Recently, artificial ribonucleases have been attracting attention, owing to their potential use as tools for gene manipulation, the control of gene expression, and others.^{2–5} In most cases, RNA-cleaving molecules are bound to the terminals of oligonucleotides, which bind to a specific sequence in the target RNA. The scission by these conjugates takes place at a limited number of sites.⁴ However, a precise prediction of the scission site is difficult, due to the dangling motion of the single-stranded portion of the substrate RNA. In addition, a wobbling of the cleaver tends to render the scission less selective.

In order to cut RNA still more selectively at a desired site, it is preferable to attach cleaving molecules inside of the DNA strands. When two portions of the DNA in these artificial enzymes form heteroduplexes with the complementary parts in the substrate RNA, the cleavers are precisely placed at the targeted position. The molecular movements of the RNA substrates

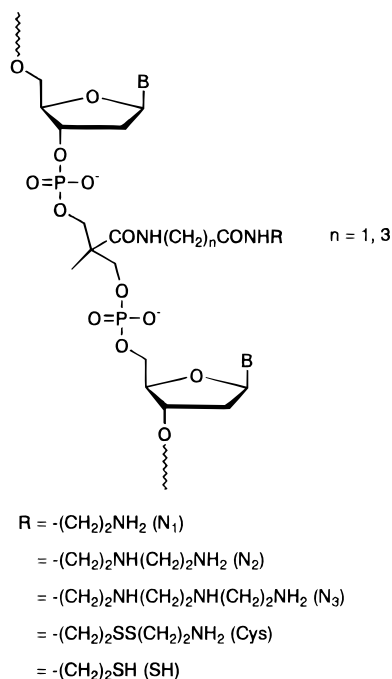


Figure 1. Modified oligonucleotides synthesized in the present study.

and artificial enzymes are suppressed in rigidly structured duplexes, thus making the scission site more predictable.

In the present study, artificial ribonucleases were prepared by interposing oligoamines (catalysts for RNA hydrolysis)⁸ between two DNA strands (see Figure 1). Novel phosphoramidite monomers (**3** and **6** in Scheme 1) having ester residues in the side chains were synthesized for this purpose. The riboses in the conventional phosphoramidite monomers were replaced by trimethylene main chains in order to minimize the steric perturbation. Oligoamines were introduced by post-reactions to the desired sites in the oligonucleotides using aminolysis of the esters. These artificial ribonucleases hydrolyzed substrate RNA at exactly the predicted site. The scission patterns are discussed in terms of the results of a computer-modeling study.

(8) Yoshinari, K.; Yamazaki, K.; Komiyama, M. *J. Am. Chem. Soc.* **1991**, *113*, 5899.

[®] Abstract published in *Advance ACS Abstracts*, January 15, 1997.

(1) A preliminary communication on the synthesis of the phosphoramidite **3**: Endo, M.; Saga, Y.; Komiyama, M. *Tetrahedron Lett.* **1994**, *35*, 5879.

(2) (a) Cech, T. R. *Science* **1987**, *236*, 1532. (b) Komiyama, M. *J. Biochem.* **1995**, *118*, 665. (c) DeMesmaeker, A.; Häner, R.; Martin, P.; Moser, H. E. *Acc. Chem. Res.* **1995**, *28*, 366.

(3) (a) Matthews, J. A.; Kricka, L. J. *Anal. Biochem.* **1988**, *169*, 1. (b) Marcus-Sekura, C. J. *Anal. Biochem.* **1988**, *172*, 289. (c) Toulmè, J.-J.; Hélène, C. *Gene* **1988**, *72*, 51. (d) Maher, L. J., III, Wold, B.; Dervan, P. B. *Science* **1989**, *245*, 725.

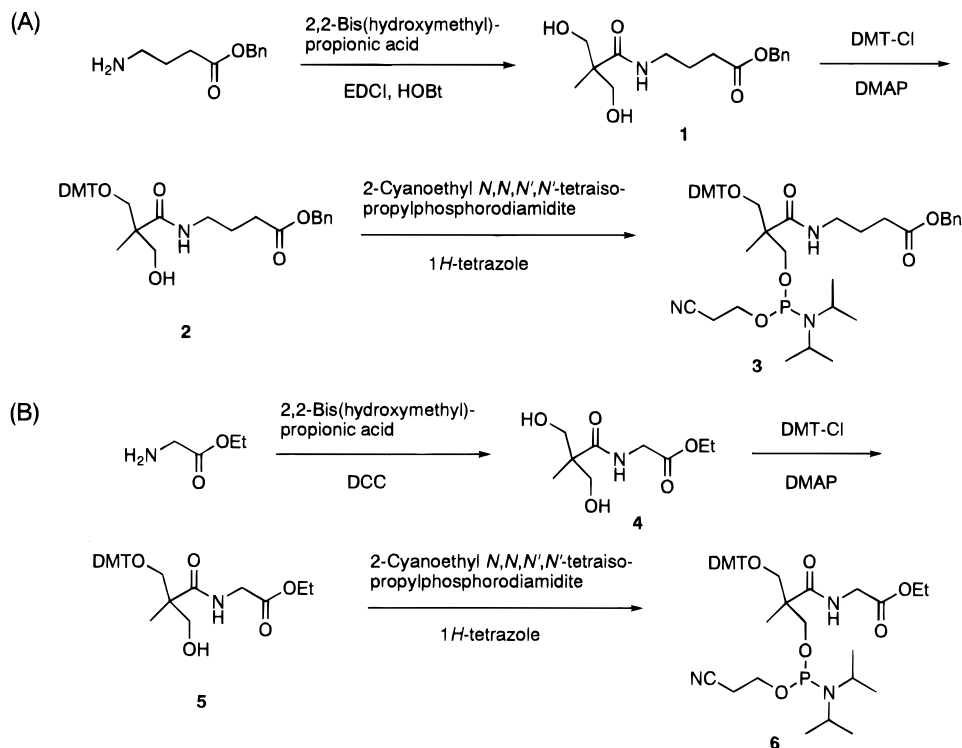
(4) (a) Zuckermann, R. N.; Schultz, P. G. *J. Am. Chem. Soc.* **1988**, *110*, 6592. (b) Matsumura, K.; Endo, M.; Komiyama, M. *J. Chem. Soc., Chem. Commun.* **1994**, 2019. (c) Bashkin, J. K.; Frolova, E. I.; Sampath, U. *J. Am. Chem. Soc.* **1994**, *116*, 5981. (d) Magda, D.; Miller, R. A.; Sessler, J. L.; Iverson, B. L. *J. Am. Chem. Soc.* **1994**, *116*, 7439. (e) Hall, J.; Hüsken, D.; Piele, U.; Moser, H. E.; Häner, R. *Chem. Biol.* **1994**, *1*, 185. (f) Uchiyama, Y.; Inoue, H.; Ohtsuka, E.; Nakai, C.; Kanaya, S.; Ueno, Y.; Ikehara, M. *Bioconjugate Chem.* **1994**, *5*, 327. (g) Komiyama, M.; Inokawa, T.; Yoshinari, K. *J. Chem. Soc., Chem. Commun.* **1995**, 77.

(5) For DNA scission by artificial nucleases, see: (a) Dervan, P. B. *Science* **1986**, *232*, 464. (b) Moser, H. E.; Dervan, P. B. *Science* **1987**, *238*, 645. (c) Sigman, D. S.; Chen, C. B. *Annu. Rev. Biochem.* **1990**, *59*, 207. (d) Nielsen, P. E. *Bioconjugate Chem.* **1991**, *2*, 1. (e) Sigman, D. S.; Bruce, T. W.; Mazumder, A.; Sutton, C. L. *Acc. Chem. Res.* **1993**, *26*, 98. (f) Thuong, N. T.; Hélène, C. *Angew. Chem., Int. Ed. Engl.* **1993**, *32*, 666. (g) Reference 2b.

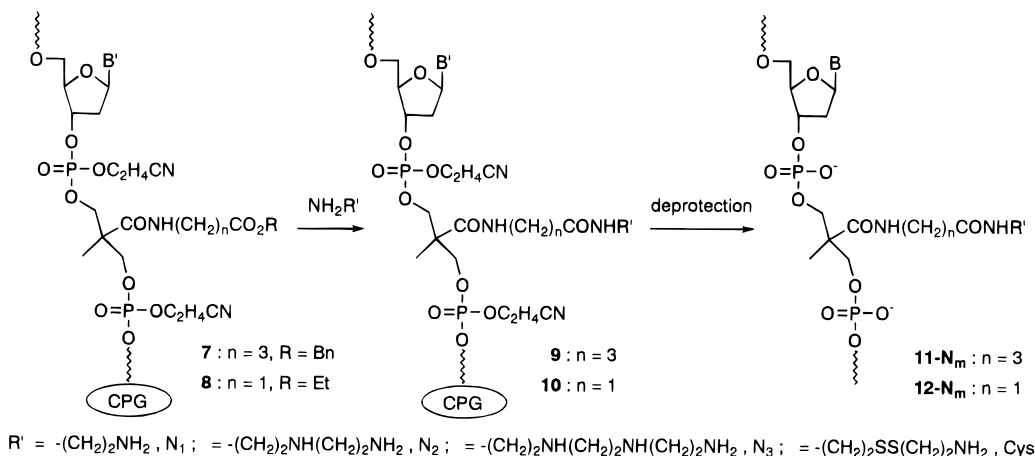
(6) (a) Uhlmann, E.; Peyman, A. *Chem. Rev.* **1990**, *90*, 543. (b) Goodchild, J. *Bioconjugate Chem.* **1990**, *1*, 165.

(7) Diastereoselective synthesis of a phosphoramidite monomer of dinucleotide, which has a reactive residue on the phosphorus atom, was reported: Endo, M.; Komiyama, M. *J. Org. Chem.* **1996**, *61*, 1994 and references therein.

Scheme 1



Scheme 2



Results

Synthesis of Phosphoramidite Monomers 3 and 6. Phosphoramidite monomer **3** was synthesized according to Scheme 1A. First, 2,2-bis(hydroxymethyl)propionic acid was condensed with benzyl 4-aminobutylate using 1-ethyl-3-[3-(dimethylamino)propyl]carbodiimide hydrochloride (EDCI). One of the two hydroxyl groups in **1** was protected by 4,4'-dimethoxytrityl chloride (DMT-Cl). The final phosphorylation was made by 2-cyanoethyl *N,N,N',N'*-tetraisopropylphosphorodiamidite and 1*H*-tetrazole. Another phosphoramidite monomer **6** was prepared in a similar way, except for the use of glycine ethyl ester and dicyclohexylcarbodiimide (DCC) in place of benzyl 4-aminobutylate and EDCI, respectively (Scheme 1B). The resultant **3** and **6** were purified by column chromatography and used for DNA synthesis.

Oligonucleotide Synthesis Using Phosphoramidite Monomers 3 and 6. By using phosphoramidite monomers **3** and **6**, various oligonucleotides (**7** and **8** in Scheme 2) were prepared on an automated DNA synthe-

size. The coupling efficiencies for the steps involving **3** and **6** were 98 and 99%, respectively, as estimated from the amount of released DMT. The benzyl and ethyl esters remained intact during DNA synthesis.

Typical prepared oligonucleotides were 5'-TCA GCC GGA TCA AXT CAT CGT-3': **7-1** (by **3**), **8-1** (by **6**) and 5'-TCA GCC GGA TCX AGT CAT CGT-3': **7-2** (by **3**) where X denotes the residue derived from **3** or **6**.

Attachment of Functional Residues to Oligonucleotides 7 and 8. Oligoamines were site-selectively introduced to **7** and **8** by aminolysis of the benzyl or ethyl ester (the first step in Scheme 2). The CPG columns used for DNA synthesis were reacted directly with various oligoamines in dry dioxane at 45 °C for 36 h. By this simple method, the desired functionalized oligonucleotides, **11-N_m** and **12-N_m**, were obtained in high yields. Here, *m* refers to the kind of oligoamine introduced. For example, the product from **7-1** and diethylenetriamine is designated as **11-1-N₂**, since an ethylenediamino residue is bound to **7-1** via an amide linkage (note that

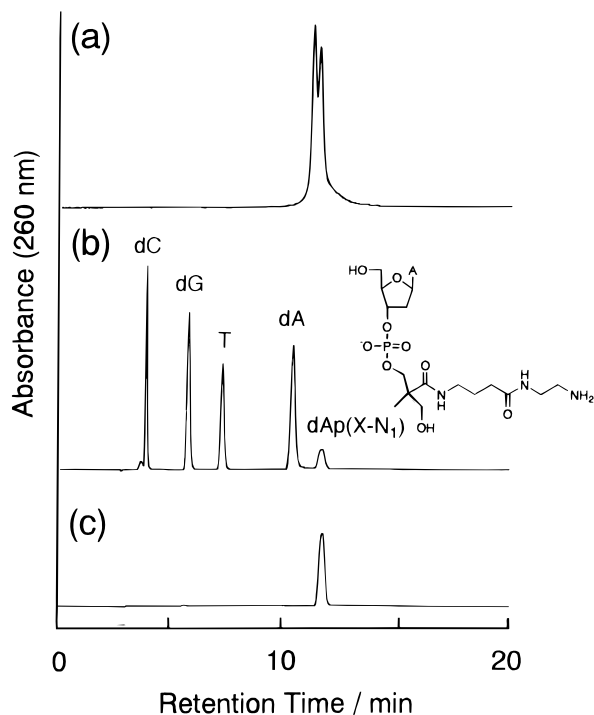


Figure 2. HPLC profiles for the oligonucleotide **11-1-N₁** (A), its enzymatically digested products (B), and authentic sample of dAp(X-N₁) (C); the enzymatic digestion was achieved by alkaline phosphatase and snake-venom phosphodiesterase.

one of the terminal amino residues of the diethylenetriamine is used to form the amide linkage).

In a similar way, a cystamine residue was introduced to **7** and **8**. These cystamine-attached oligonucleotides (**11-Cys** and **12-Cys**) were further converted to the corresponding thiol-attached ones (**11-SH** and **12-SH**) by reducing the disulfide linkage with dithiothreitol (DTT) at pH 8.⁹

When **11-1-N₁** was digested by alkaline phosphatase and snake-venom phosphodiesterase, dAp(X-N₁), in which an amino residue is bound to X in dApX via an amide linkage, was formed together with the common four deoxynucleosides (Figure 2b). The ratio (dA:dC:dG:T:dAp(X-N₁)) = 4:6:4:5:1 was exactly identical to the theoretical one. The peak for dAp(X-N₁) could be concretely assigned by coinjection with its authentic sample, which was prepared independently. The phosphodiester linkage in dAp(X-N₁) was resistant to enzymatic digestion. Furthermore, a trimer dApXpT was reacted with triethylenetetramine under the conditions employed for the aminolysis of the oligonucleotides, and the product was analyzed by mass spectroscopy. As expected, the signals for dAp(X-N₃)pT were observed (see the Experimental Section).

Site-Selective RNA Scission by Oligonucleotides 11-1-N₃ and 11-2-N₃. Figure 3A shows the polyacrylamide gel electrophoresis pattern for RNA hydrolysis by **11-1-N_m**. The two DNA portions in these conjugates are complementary to the substrate 28-mer RNA at the A₃-A₉ and the U₁₁-A₂₃ parts, respectively. When **11-1-N₃** was used, the scission selectively occurred at the C₁₀-U₁₁ and the U₁₁-U₁₂ linkages (lane 6: the scission profile is presented in Figure 4). These scission sites were located just in front of the diethylenetriamino residue, when **11-1-N₃** and the substrate RNA formed hetero-

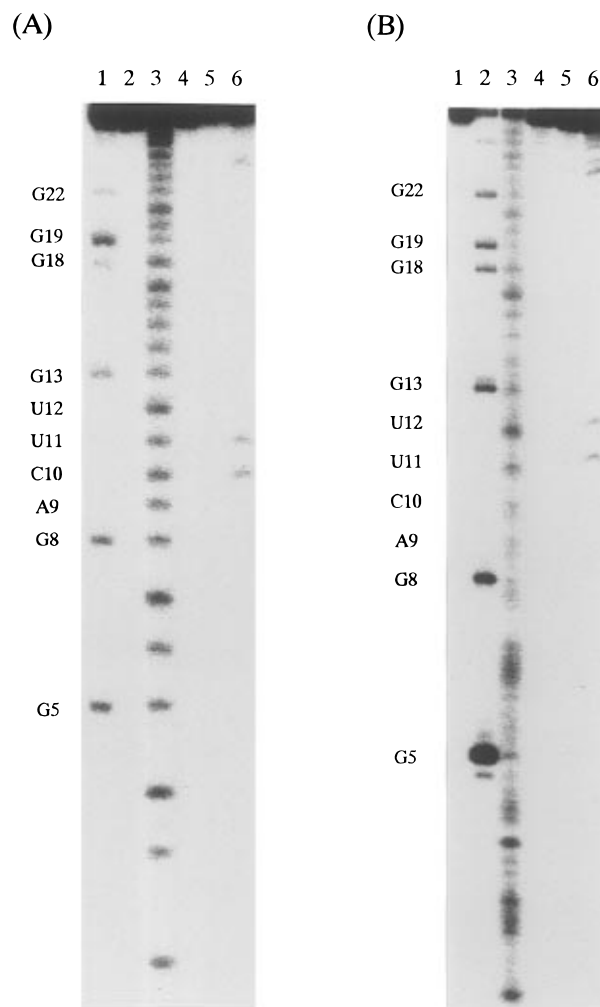


Figure 3. Autoradiographs of 20% denaturing polyacrylamide gel electrophoresis for the hydrolysis of 28-mer RNA (³²P-labeled at the 5'-end) by **11-1-N_m** (A) and by **11-2-N_m** (B). A: lane 1, ribonuclease T₁ (G-specific); lane 2, no treatment; lane 3, alkaline hydrolysis; lane 4, **11-1-N₁**; lane 5, **11-1-N₂**; lane 6, **11-1-N₃**. B: lane 1, no treatment; lane 2, ribonuclease T₁; lane 3, alkaline hydrolysis; lane 4, **11-2-N₁**; lane 5, **11-2-N₂**; lane 6, **11-2-N₃**. Reaction conditions: 0.2 mM RNA, 20 mM artificial ribonuclease, 37 °C, 16 h, 50 mM Tris buffer (pH 7.5 for A and 8.5 for B), 10 mM EDTA. The cleavage efficiencies increased with the reaction time and at 16 h were 3% for **11-1-N₃** (lane 6 in A) and 1% for **11-2-N₃** (lane 6 in B).

5'-T CAG CCG GAT CAA XTC ATC GT-3' (**11-1-N₃**)

5'-T CAG CCG GAT CXA GTC ATC GT-3' (**11-2-N₃**)

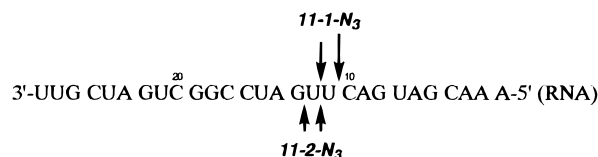


Figure 4. Scission profiles for the RNA hydrolysis by the artificial ribonucleases **11-1-N₃** and **11-2-N₃**; X denotes the residue carrying an N₃ residue. The scission sites are shown by the arrows.

duplexes (see the result of the molecular-modeling study presented in Figure 6A).

RNA hydrolysis by another artificial ribonuclease **11-2-N₃** also took place selectively in front of the diethylenetriamino residue (see lane 6 in Figure 3B and Figure 4, as well as Figure 6B). In contrast, none of

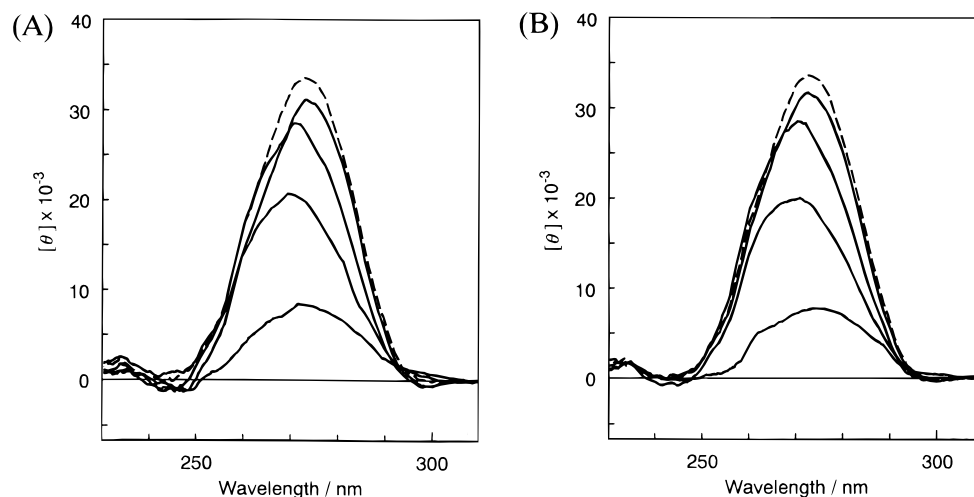


Figure 5. CD spectra of duplexes of the modified oligonucleotides **11-1-N₃** (A) and **11-2-N₃** (B) with the complementary RNA. The concentration of the complementary RNA was varied as 0, 1, 2, and 3 mM (from the bottom), with the concentrations of the modified oligonucleotide kept constant at 3 mM. The dotted lines are for the duplexes between the unmodified DNA (3 mM) and the complementary RNA (3 mM). Measurement conditions are presented in the Experimental Section.

the **11-1-N₁**, **11-1-N₂**, **11-2-N₁**, and **11-2-N₂** was active for RNA hydrolysis (lanes 4 and 5 for both A and B in Figure 3).¹⁰ The N₃ residues are essential for RNA scission.

Structures of the Duplexes of 11-1-N₃ and 11-2-N₃. The circular dichroism (CD) spectra of the duplexes of modified oligonucleotides **11-1-N₃** and **11-2-N₃** with the complementary RNA are presented in Figure 5. Apparently, all the heteroduplexes take typical A-type conformations in a wide range of molar ratio of the modified DNA to the RNA.¹¹ Furthermore, the spectra for the heteroduplexes of the modified oligonucleotides are nearly identical with the ones for the corresponding duplexes between the unmodified DNA and the complementary RNA (the dotted lines in Figure 5). The chemical modification of the oligonucleotides does not cause any drastic distortion of the duplexes with the complementary RNA.

Thermal Stabilities of the Duplexes of the Modified Oligonucleotides. The melting temperatures (T_m 's) of the duplexes between the modified oligonucleotides, prepared in the present study, and either the complementary DNA or RNA are summarized in Table 1. In all cases, the T_m 's are higher than 50 °C. Thus, the duplexes can be satisfactorily formed under the physiological conditions.

Molecular Modeling on the Heteroduplexes of Artificial Ribonucleases with the Substrate RNA. According to molecular modeling, the heteroduplex of **11-1-N₃** with the RNA substrate is most stable when the N₃ residue (the catalytic site) is located near the phosphodiester linkage between the C10 and the U11 residues (C10-p-U11) of the RNA; the corresponding structure is depicted in Figure 6A, and the potential energies are presented in Table 2. The placement of the N₃ residue at the U11-p-U12 linkage, another scission site, also provides a stable structure. In the heteroduplex of **11-2-N₃** with the RNA, the U12-p-G13 linkage (the selective scission site) is the most favorably accessible

(10) The selective hydrolysis was accompanied by some additional scissions near the 3'-end. Assumedly, these linkages are activated for alkaline hydrolysis on the hetero-duplex formation.

(11) Allen, F. S.; Gray, D. M.; Roberts, G. P.; Tinoco, I., Jr. *Biopolymers* **1972**, *11*, 853.

Table 1. Melting Temperatures (T_m , °C) of the Duplexes between the Modified Oligonucleotides and Their Complementary DNA and RNA^{a,b}

complementary strand	modified oligonucleotide			
	Z	11-1-Z	11-2-Z	12-1-Z
DNA	N ₁	53.3	55.8	53.1
	N ₂	54.2	57.1	54.2
	N ₃	55.4	57.3	54.4
	Cys	56.3		54.5
	SH	50.7 ^c		52.9 ^c
RNA	N ₃	52.1 ^d	55.4 ^d	

^a The complementary strand is 5'-GCTAAACGATGACTTGATC-CGGCTGATCGTC-3' for DNA/DNA complexes and 5'-AAAAC-GAUGACUUGAUCCGGCUGAAAAAAC-3' for DNA/RNA complexes. T_m 's were measured in pH 7 solutions containing 1 μM DNA (or RNA), 10 mM sodium cacodylate, and 100 mM NaCl. Measurement error is estimated to be <0.5 °C. ^b T_m of the unmodified DNA/DNA duplex is 65.6 °C, and the corresponding value for the DNA/RNA complex is 63.3 °C. ^c 0.1 mM DTT was added to the solutions. ^d 1 mM EDTA was added to the solutions.

site (Figure 6B). Selective scission by the artificial enzymes (Figures 3 and 4) occurs at the positions where the N₃ residue is accessible without causing much instability in the duplexes.¹²

Discussion

Interposition of an RNA Cleaver between Two DNA Oligomers for a Pinpoint Scission. As clearly evidenced above, an RNA cleaver, interposed between two DNA oligomers, can be precisely placed at the targeted phosphodiester linkage in substrate RNA. The molecular movements of both the cleaver and the phosphodiester linkage are marginal in heteroduplexes. Under these conditions, predicting the scission site is

(12) The calculation on the duplex of **11-2-N₃** indicates that the G13-p-A14 and A14-p-U15 linkages are more accessible by N₃ than the U11-p-U12 linkage (the latter linkage is another scission site). Probably, structural changes of the strand around the X-residue cannot be satisfactorily reproduced by the present calculation.

(13) Alternatively, the simultaneous protonation of both of the two amino residues might be responsible for the lack of activities. Although the pK_a values of free ethylenediamine are 6.7 and 9.5, they can be increased by negative charges of the DNA and RNA when the artificial ribonucleases form heteroduplexes with the substrate RNA. Here, the acid-base cooperation cannot operate.

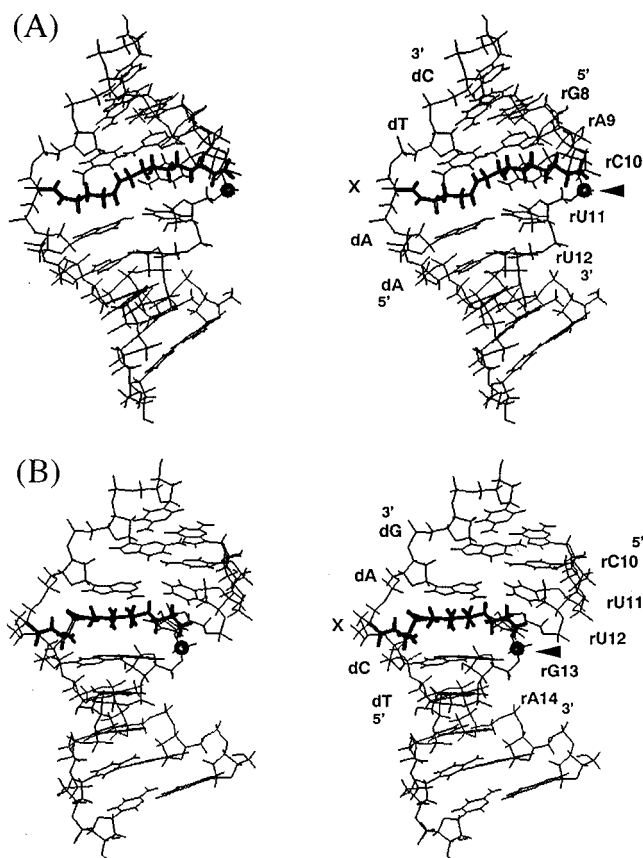


Figure 6. Stereoviews of the most stable structures of the duplexes of the substrate RNA with **11-1-N₃** (A) and **11-2-N₃** (B): the bold line shows the side chain containing the diethylenetriamine N₃, whereas the hydrolyzed phosphodiester linkage is indicated by the circle with an arrow. The calculation was made using the Biosym Insight II/Discover program on nine residues for the artificial ribonuclease and the RNA. The assumptions employed for the calculation are presented in the Experimental Section.

Table 2. Total Potential Energy (kcal/mol) for the Heteroduplexes between the Modified Oligonucleotides and the Complementary RNA, in which the Terminal Amino Residues in N₃ are Placed at the Corresponding Phosphodiester Linkage^a

11-1-N₃		11-2-N₃	
phosphodiester linkage	potential energy	phosphodiester linkage	potential energy
A9-C10	-5597	C10-U11	-5674
C10-U11 ^b	-5797	U11-U12 ^b	-5724
U11-U12 ^b	-5677	U12-G13 ^b	-5921
U12-G13	-5642	G13-A14	-5859

^a Calculation was made for 9-mer heteroduplexes (d(ATCAAX-TCA)/r(UGACUUGAU) for **11-1-N₃** and d(GGATCXAGT)/r(ACU-UGAUCC) for **11-2-N₃**) (see Experimental Section for details).

^b The hydrolyzed phosphodiester linkages.

straightforward. Undoubtedly, this is a great advantage of the present artificial ribonucleases over the previous ones (see Introduction) from the viewpoint of practical applications.

Phosphoramidite monomers **3** and **6** are eminent for preparing these artificial ribonucleases. Both of them provide three carbon atoms to the backbone of the oligonucleotides, as do the common phosphoramidite monomers. A less bulky and flexible trimethylene residue is used to minimize the steric hindrance. In addition to oligoamines, various functional residues are easily (and

in high yields) incorporated into the desired sites of oligonucleotides using aminolysis of the esters. According to CD spectroscopy (Figure 5) and T_m measurements (Table 1), these modified oligonucleotides form stable duplexes with RNA under the physiological conditions without any significant structural distortion. Strong potentialities of the present synthetic method have been indicated.

The incorporation of RNA cleaver between two DNA oligomers can be also advantageous to achieve catalytic turnover. When the substrate RNA is cleaved at the inside of strand, the fragments are spontaneously removed from the artificial ribonucleases since the melting temperatures of their duplexes with the complementary DNA portions are lower.

Mechanism of RNA Hydrolysis and Molecular Modeling. The N₃ residues in **11-1-N₃** and **11-2-N₃** are essential for RNA hydrolysis. The cleavage occurs at the phosphodiester linkage, which the N₃ can approach favorably, as indicated by the molecular modeling. Probably, a neutral amino residue and an ammonium cation show intramolecular acid-base cooperation.⁸ Under the reaction conditions, two of the amino residues in N₃ are protonated and the other (the central one) is in a neutral form.¹⁴ Consistently, **11-1-N₂** and **11-2-N₂** are inactive (lanes 5 in Figure 3 A,B). It is sterically difficult to place both of the two amino residues in the ethylenediamine near the phosphodiester linkage.¹³ The argument is further supported by the absence of the catalytic activities of **11-1-N₁** and **11-2-N₁** (lanes 4), since no intramolecular acid-base cooperation takes place there.

Ethylenediamine tetraacetate (EDTA), a well-known metal-ion chelator, showed no effect on selective scission. The possibility that metal ions, if any, in the reaction mixtures participate in the RNA hydrolysis is ruled out (all the RNA hydrolyses in Figure 3 were achieved in the presence of 10 mM EDTA). Note that contamination by metal ions was carefully avoided by using highly purified water (the specific resistance > 18.3 MΩ) as the solvent.

Conclusion

Phosphoramidite monomers **3** and **6** are very useful for attaching various functional residues inside of DNA strands. When these modified oligonucleotides form duplexes with the complementary nucleic acids, the positions of the functional residues are precisely controlled, and thus, the reactions take place selectively at the target sites. The site-selective RNA hydrolyses exhibited in Figures 3 and 4 are typical examples of the application. It is noteworthy that the scission sites are identical with the sites predicted by a molecular-modeling study. The scission efficiencies should be improved by a more precise molecular design. These artificial enzymes are valuable for molecular biology, biotechnology, therapy, and others, since the scission sites are highly restricted and predicted. These attempts are currently under way in our laboratory.

Experimental Section

Materials. 2-Cyanoethyl *N,N,N,N*-tetraisopropylphosphorodiamidite and triethylenetetramine were obtained from Aldrich. 2,2-Bis(hydroxymethyl)propionic acid, cystamine hy-

(14) The pK_a values of diethylenetriamine are 4.6, 8.6, and 9.7, as determined by potentiometric titration (protonation of the central amine is greatly suppressed by the electrostatic repulsion by the neighboring two positive charges).

drochloride, DCC, 4-(dimethylamino)pyridine (DMAP), EDCI, glycine ethyl ester hydrochloride, and 1*H*-tetrazole, as well as ethylenediamine and diethylenetriamine, were purchased from Tokyo Kasei. 3-Hydroxybenzotriazole (HOBt) was obtained from Wako, and DMT-Cl was from Dojin. 1,4-Dioxane and pyridine were distilled from metallic sodium and potassium hydroxide, respectively. Acetonitrile, CH₂Cl₂, DMF, and the oligoamines were dried over molecular sieves (4 Å). The conventional phosphoramidite agents (Expedite) were purchased from PerSeptive Biosystems. Silica gel column chromatography was achieved using Kieselgel 60 from Merck, and TLC was performed on precoated silica gel plates (Merck Kieselgel 60 F254). The enzymes used were alkaline phosphatase and snake-venom phosphodiesterase from Boehringer Mannheim, and T4 polynucleotide kinase was from Nippon Gene.

The substrate 28-mer RNA was prepared on a DNA synthesizer and purified in the recommended fashion.¹⁵ The choice of sequence was arbitrary. The RNA was labeled at the 5'-end by adenosine [γ -³²P]triphosphate (from Amersham) with T4 polynucleotide kinase and purified by polyacrylamide gel electrophoresis.

Benzyl 4-[*N*-[2,2-Bis(hydroxymethyl)propionyl]amino]butylate (1). EDCI (3.00 g, 15.6 mmol) was added to a mixture of benzyl 4-aminobutylate (2.99 g, 13.0 mmol), 2,2-bis(hydroxymethyl)propionic acid (2.09 g, 15.6 mmol), HOBt (2.12 g, 15.6 mmol), triethylamine (2.72 mL, 19.5 mmol), and DMF (10 mL). After the mixture was stirred for 12 h at room temperature, the solvent was removed, and 100 mL of ethyl acetate was poured. The organic layer was washed with 100 mL of saturated aqueous solutions of NaHCO₃ (once) and of NaCl (twice), dried over anhydrous Na₂SO₄, and concentrated under reduced pressure. The product was purified by silica gel column chromatography (CH₂Cl₂:MeOH = 95:5) to afford 2.84 g of **1** (63% yield): ¹H-NMR [CDCl₃(TMS)] δ 7.33 (brs, 5H), 7.02 (brs, 1H), 5.10 (s, 2H), 3.67 (d, *J* = 4.0 Hz, 4H), 3.26 (q, *J* = 5.9 Hz, 2H), 3.07 (t, *J* = 5.0 Hz, 2H), 2.39 (t, *J* = 7.6 Hz, 2H), 1.84 (quin, *J* = 6.9 Hz, 2H), 1.05 (s, 3H); *R*_f = 0.28 (CH₂Cl₂:MeOH = 10:1).

Benzyl 4-[*N*-[2-[(4,4'-Dimethoxytrityl)oxy]methyl]-2-(hydroxymethyl)propionyl]amino]butylate (2). A dry pyridine solution (10 mL) of **1** (2.84 g, 8.22 mmol) and DMAP (53 mg, 0.41 mmol) was cooled on ice under nitrogen, and DMT-Cl (3.34 g, 9.86 mmol) in 5 mL of CH₂Cl₂ was added dropwise. After 12 h, 100 mL of CH₂Cl₂ was poured into the mixture. The CH₂Cl₂ layer was dried with anhydrous Na₂SO₄ after being washed with saturated aqueous solutions of NaHCO₃ (twice) and of NaCl (once). Silica gel column chromatography (CH₂Cl₂:*i*-PrOH:Et₃N = 97.5:2.5:1) gave 4.87 g of **2** (59% yield): ¹H-NMR [CDCl₃(TMS)] δ 7.20–7.41 (m, 14H), 7.04 (brt, 1H), 6.83 (d, *J* = 8.6 Hz, 4H), 5.09 (s, 2H), 3.77 (s, 6H), 3.59 (d, *J* = 6.6 Hz, 2H), 3.20–3.32 (m, 4H), 2.35 (t, *J* = 7.6 Hz, 2H), 1.81 (quin, *J* = 7.2 Hz, 2H), 1.19 (s, 3H); *R*_f = 0.19 (CH₂Cl₂:*i*-PrOH:Et₃N = 97.5:2.5:1).

Phosphoramidite Monomer 3. In a dry acetonitrile solution (10 mL), **2** (0.28 g, 0.45 mmol) and 2-cyanoethyl *N,N,N,N*-tetraisopropylphosphorodiamidite (0.16 mL, 0.50 mmol) were reacted with 1*H*-tetrazole (35 mg, 0.50 mmol) under nitrogen. Prior to the reaction, **2** and 1*H*-tetrazole were dried by coevaporation with dry acetonitrile (twice). After 1 h, the product was taken into 100 mL of ethyl acetate. The organic solution was washed with 100 mL of saturated aqueous solutions of NaHCO₃ and of NaCl, dried over Na₂SO₄, and desalted; finally, the solvent was removed *in vacuo*. The resultant product was purified by silica gel column chromatography (hexane:AcOEt = 3:1) to afford 0.22 g of phosphoramidite **3** (67% yield): ¹H-NMR [CDCl₃(TMS)] δ 7.19–7.44 (m, 14H), 6.82 (d, *J* = 8.6 Hz, 4H), 5.08 (s, 2H), 4.11 (q, *J* = 6.9 Hz, 2H), 3.76 (s, 6H), 3.68 (m, 2H), 3.51 (m, 2H), 3.24 (m, 4H), 2.73 (m, 1H), 2.48 (q, *J* = 5.9 Hz, 2H), 2.33 (t, *J* = 7.6 Hz, 2H), 1.76 (quin, *J* = 7.6 Hz, 2H), 1.07–1.29 (m, 15H); ³¹P-NMR (CDCl₃) δ 152.37, 152.41; *R*_f = 0.59 (hexane:AcOEt = 1:1).

Ethyl 2-[*N*-[2,2-Bis(hydroxymethyl)propionyl]amino]ethylate (4). Triethylamine (6.95 mL, 50 mmol) was added to glycine ethyl ester hydrochloride (7.00 g, 50 mmol) in 25 mL of DMF, and the formed triethylammonium hydrochloride was filtered out. To the filtrate was added 2,2-bis(hydroxymethyl)propionic acid (7.40 g, 55 mmol); then, DCC (11.4 g, 55 mmol) in 20 mL of dioxane was slowly dropped into this mixture on ice. The mixture was stirred for 12 h at room temperature and filtered again. The filtrate was concentrated under reduced pressure and purified by silica gel column chromatography (CH₂Cl₂:*i*-PrOH = 100:5), giving 8.19 g of **4** (75% yield): ¹H-NMR [CDCl₃(TMS)] δ 7.68 (brt, 1H), 4.12 (q, *J* = 7.2 Hz, 2H), 4.05 (d, *J* = 5.9 Hz, 2H), 3.79 (brs, 6H), 1.29 (t, *J* = 7.2 Hz, 3H), 1.09 (s, 3H); *R*_f = 0.11 (CH₂Cl₂:*i*-PrOH = 100:5).

Ethyl 2-[*N*-[2-[(4,4'-Dimethoxytrityl)oxy]methyl]-2-(hydroxymethyl)propionyl]amino]ethylate (5). A CH₂Cl₂ solution (10 mL) of **4** (5.58 g, 21.8 mmol), DMAP (0.12 g, 1.0 mmol), and *N,N*-diisopropylethylamine (5.2 mL, 30 mmol) was cooled on ice under nitrogen, and DMT-Cl (6.78 g, 20 mmol) in 10 mL of CH₂Cl₂ was dropwise added. After 12 h, the product was treated as for **2**, and purified by silica gel column chromatography (CH₂Cl₂:*i*-PrOH = 100:2). The yield was 4.80 g (43%): ¹H-NMR [CDCl₃(TMS)] δ 7.18–7.43 (m, 9H), 6.84 (d, *J* = 8.9 Hz, 4H), 4.19 (q, *J* = 7.3 Hz, 2H), 4.00 (dd, *J* = 4.3, 5.6 Hz, 2H), 3.80 (s, 6H), 3.64 (d, *J* = 6.6 Hz, 2H), 3.30 (dd, *J* = 9.2, 23.4 Hz, 2H), 2.35 (t, *J* = 7.3 Hz, 2H), 1.18 (s, 3H); *R*_f = 0.39 (CH₂Cl₂:MeOH = 95:5).

Phosphoramidite Monomer 6. In 10 mL of dry acetonitrile, **5** (0.52 g, 1.0 mmol) and 2-cyanoethyl *N,N,N,N*-tetraisopropylphosphorodiamidite (0.35 mL, 1.1 mmol) were treated with 1*H*-tetrazole (77 mg, 1.1 mmol) under nitrogen for 1 h. After the usual workup, the mixture was dried over Na₂SO₄ and purified by silica gel column chromatography (hexane:AcOEt = 3:1) to give 0.33 g of the phosphoramidite **6** (52% yield): ¹H-NMR [CDCl₃(TMS)] δ 7.18–7.43 (m, 9H), 6.82 (d, *J* = 8.9 Hz, 4H), 4.17 (q, *J* = 6.9 Hz, 2H), 3.96 (q, *J* = 5.3 Hz, 2H), 3.79 (s, 6H), 3.66–3.75 (m, 4H), 3.55 (m, 2H), 3.29 (m, 2H), 2.54 (m, 2H), 1.08–1.28 (m, 18H); ³¹P-NMR (CDCl₃) δ 154.03, 154.07; *R*_f = 0.54 (hexane:AcOEt = 1:1).

Synthesis of Modified Oligonucleotides 7 and 8. By using phosphoramidite monomers **3** and **6**, together with the conventional Expedite agents, various oligodeoxyribonucleotides were automatically synthesized on a MilliGen/Biosearch Cyclone Plus DNA synthesizer. The concentrations (52 mM) of **3** and **6** in dry acetonitrile were 1.5 times as large as those used for the Expedite agents.

Attachment of Amino Compounds to 7 and 8. After DNA synthesis, the CPG column was kept in 1.5 mL of a 1:2 mixture of the amine and dioxane at 45 °C for 36 h and then treated with concentrated NH₄OH for 1 h at room temperature. The oligonucleotide (with the DMT on) was purified by reversed-phase HPLC and further treated with a 4:1 mixture of acetic acid and acetonitrile for 1 h. The final purification was also carried out by HPLC (conditions: 5–20% acetonitrile/water (20 min), 50 mM ammonium formate, 260 nm, 1.0 mL/min).

In order to both measure the concentrations of these oligonucleotides and to confirm their structures, they were hydrolyzed by alkaline phosphatase and snake-venom phosphodiesterase at pH 7.0 and 37 °C for 2 h. The digests were analyzed by reversed-phase HPLC: 5–10% acetonitrile/water (20 min) for **11-1-N_m**, **11-2-N_m** and **12-1-N_m**, and 5–20% (20 min) for the others.

Preparation of an Authentic Sample of dAp(X-N₁). The Expedite agent for dA (*N*⁶-(*tert*-butylphenoxyacetyl)-5'-*O*-(4,4'-dimethoxytrityl)-2'-deoxyadenosine 3'-*O*-(2-cyanoethyl *N,N*-diisopropylphosphoramidite)) (100 mg, 0.106 mmol) and **2** (65 mg, 0.106 mmol) were reacted with 1*H*-tetrazole (24 mg, 0.32 mmol) in 10 mL of acetonitrile under nitrogen for 1 h at room temperature. Then, iodine (40 mg, 0.16 mmol) in 5 mL of THF and 1 mL of 2,6-lutidine were added to the mixture. After 30 min, the mixture was concentrated and dissolved in 100 mL

(15) Gait, M. J.; Pritchard, C.; Slim, G. *Oligonucleotides and Analogues*; Eckstein, F., Ed.; IRL Press: Oxford, 1991; p 25.

of CH_2Cl_2 . The organic layer was washed with 100 mL of saturated aqueous solutions of $\text{Na}_2\text{S}_2\text{O}_3$ and of NaHCO_3 and dried over Na_2SO_4 . Silica gel column chromatography (CH_2Cl_2 :MeOH:Et₃N = 100:10:1) afforded the fully protected dApX in 25% yield (38 mg).

The protected dApX was incubated in 1.5 mL of a 1:2 mixture of ethylenediamine and dioxane at 40 °C for 48 h. The product was successively treated with 29% NH_4OH for 1 h at room temperature and then with 4:1 acetic acid–acetonitrile solution for 1 h. The product was dissolved in water, filtered, and purified by HPLC [5–20% acetonitrile/water (20 min) containing 50 mM ammonium formate]: ¹H-NMR [D_2O (TSP)] δ 8.34 (s, 1H), 8.25 (s, 1H), 6.51 (t, $J = 6.3$ Hz, 1H), 4.37 (q, $J = 2.3$ Hz, 1H), 4.01 (m, 1H), 3.84–3.90 (m, 4H), 3.77 (d, $J = 11.0$ Hz, 1H), 3.62 (d, $J = 11.0$ Hz, 1H), 3.48 (t, $J = 5.6$ Hz, 2H), 3.24 (q, $J = 6.3$ Hz, 2H), 3.15 (q, $J = 5.9$ Hz, 2H), 2.84–2.90 (m, 1H), 2.73–2.76 (m, 1H), 2.28 (t, $J = 7.6$ Hz, 2H), 1.77 (t, $J = 7.6$ Hz, 2H), 1.24 (s, 3H); electrospray ionization mass spectroscopy (ESI-MS) m/z 573.9 [$\text{M} - \text{H}$]⁻.

Preparation of the Product of dApXpT with Triethylenetetramine by Solid-Phase Synthesis. An authentic sample of dApXpT, prepared on a DNA synthesizer, was kept in 1.5 mL of a 1:2 mixture of triethylenetetramine, and dioxane at 45 °C for 36 h. After being treated with 29% NH_4OH for 1 h and concentrated, the product was purified by reversed-phase HPLC: ESI-MS m/z 963.3 [$\text{M} - \text{H}$]⁻, 965.3 [$\text{M} + \text{H}$]⁺, 987.3 [$\text{M} + \text{Na}$]⁺.

Melting Temperature Measurements. The melting profiles of the duplexes were obtained at 260 nm in a quartz cell of 1 cm path length fitted with a Teflon stopper. The heating rate was 0.5 °C/min. The specimens contained modified oligonucleotide (1 μM), complementary DNA (1 μM), and NaCl (100 μM) in pH 7.0 cacodylate buffers (10 mM). In the case of **11-1-SH** and **12-1-SH**, 0.1 mM DTT was added to the solutions in order to avoid oxidation of the thiol residues. For the DNA/RNA heteroduplexes, 1 mM EDTA was added. The experimental error in T_m was estimated to be within 0.5 °C.

Spectroscopy. CD spectra were obtained on a JASCO J-500A spectropolarimeter at 15 °C in pH 8 solutions containing modified DNA (3 μM), complementary 32 mer RNA (0, 1, 2, and 3 μM), Tris-HCl (10 mM), NaCl (100 mM), and EDTA (1 mM). ¹H-NMR spectra (with TMS or TSP as internal standard) and ³¹P-NMR spectra (85% H_3PO_4 in D_2O as external standard) were recorded on a JEOL EX-270 NMR spectrometer at 270 and 109.4 MHz, respectively.

Sequence-Selective Hydrolysis of RNA by the Oligoamine-Attached Oligonucleotides. 5'-³²P-end-labeled 28-mer RNA (0.2 mM) was reacted in Tris buffers (50 mM) containing 20 mM artificial ribonuclease and 10 mM EDTA. After 16 h at 37 °C, the reaction mixture was analyzed on 20% denatured polyacrylamide gel. Quantification of RNA cleavage was carried out on a Fujix BAS 1000 bioimaging analyzer.

Molecular Modeling Study. Optimized modeling on duplexes of the artificial enzymes and the substrate RNA was performed using Biosym Insight II/Discover software. The following assumptions were made: (1) The heteroduplexes have A-type conformations (see the CD spectra in Figure 5). (2) The central carbon atoms of the trimethylene residues, derived from **3**, take S-type configurations. (3) The tethers are accommodated in the minor groove. (4) The distance between the nonbonding oxygen of the phosphodiester linkage and the primary nitrogen of N_3 is restrained at 3.0 Å, whereas the distance between the hydrogen in the 2'-OH of the ribose (in the 5'-side of the scission site) and the secondary nitrogen of N_3 is kept constant at 1.8 Å. The fourth assumption was made in terms of the catalytic mechanism in which one of the amino residues abstracts a proton from the 2'-OH and the adjacent ammonium ion acts as a general acid catalyst.⁸ Under these assumptions, the minimum energies (1000 steps) were calculated for each of the phosphodiester linkages of the substrate RNA, where a 5 Å layer of water molecules on the surface of the duplex was taken into consideration.

Acknowledgment. The authors are grateful to Japan Spectroscopic Co., Ltd. (JASCO, Tokyo) for measuring the mass spectra. This work was partially supported by the Ministry of Education, Science and Culture: Large-scale Research Project under the New Program System in Grants-in-Aid for Scientific Research. The award of a JSPS Research Fellowship for Young Scientists to M.E. is also acknowledged.

Supporting Information Available: ¹H NMR spectra for **1-6** and dAp(X-N₁), ³¹P-NMR spectra for **3** and **6**, and mass spectra for dAp(X-N₁) and dAp(X-N₃)pT (6 pages). This material is contained in libraries on microfiche, immediately follows this article in the microfilm version of the journal, and can be ordered from the ACS; see any current masthead page for ordering information.

JO9611780